
PROPERTIES OF A PHENYL-SUBSTITUTED POLYPHENYLENE IN DILUTE SOLUTION

JAMES L. WORK,* GUY C. BERRY, and
EDWARD F. CASASSA†

*Department of Chemistry, Carnegie-Mellon University, Pittsburgh,
Pennsylvania 15213*

JOHN K. STILLE‡

*Department of Chemistry, The University of Iowa,
Iowa City, Iowa 52240*

SYNOPSIS

Three preparations of a phenyl-substituted polyphenylene were fractionated and studied in solution by light scattering, osmometry, viscometry, fluorescence depolarization, and exclusion chromatography. Three of the five main-chain phenylene groups in the repeat unit are linked para, but the other two may be either meta or para, with the latter linkage predominating. The data are consistent with a chain structure characterized by rigid segments about 70–75 Å long, on the average, joined with 120° bond angles, about which virtually free rotation is allowed. For chains of up to about 250 backbone phenylene units, the hydrodynamic behavior in tetrahydrofuran, and other solvents, is that of a freely draining coil with intrinsic viscosity proportional to molecular weight. The effect of intramolecular excluded volume on chain conformation is negligible, although intermolecular interactions are reflected by a positive second virial coefficient (in tetrahydrofuran). Study of polymers of higher molecular weight is hampered by formation of what appear to be metastable aggregates resembling randomly branched chains.

INTRODUCTION

Certain polymers synthesized in recent years are characterized by long, relatively bulky, inflexible backbone elements. Though these units may be linked together by single bonds that allow sufficiently long chains to assume the gross conformation of a flexible coil, the polymers typically exhibit limited solubility, are soluble only in protonated form in strong acids, and are intensely colored.

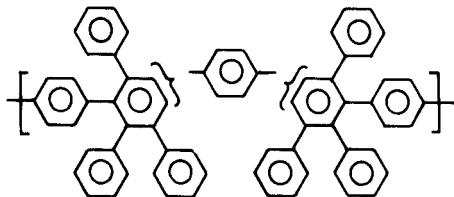
* Present address: Armstrong Cork Company, Lancaster, Pennsylvania 17604.

† To whom inquiries may be addressed.

‡ Present address: Department of Chemistry, Colorado State University, Fort Collins, Colorado 80523.

These properties make detailed study of dilute solutions difficult or impossible and frustrate comparison with theory for the behavior of the more familiar flexible chains.

We, therefore, considered it of interest to study a substituted polyphenylene that gives nearly colorless solutions in a variety of ordinary organic solvents [1] and yet has long rodlike segments in the chain backbone. The structure incorporate five backbone phenylene rings per repeat unit:



Three of the five are linked para, but the second and fourth, as shown above, can be either para or meta. Studies on formation of model compounds suggest that the alternative catenations are about equally probable [2]. Lack of steric hindrance at the link between repeat units renders the chain flexible in the sense that rotational isomerization is possible for any chain with more than one meta linkage.

In the following we report dilute solution measurements on fractionated polymer and explore correlations among the results from exclusion chromatography, osmotic pressure, light scattering, intrinsic viscosity, and fluorescence depolarization.

EXPERIMENTAL

Materials

A Diels-Alder step-growth reaction was used to obtain the polymer. The synthesis, from the preparation and purification of the monomer, is described elsewhere [2, 3]. The polymer was fractionated by precipitation from chloroform solution (1.0 g/liter) by addition of methanol. The nonsolvent was added slowly to bring the stirred solution to the cloud point. The solution was heated until it was again clear; a small additional amount of solvent was added; and then the solution was cooled slowly to the original temperature, whereupon agitation was stopped and the precipitated polymer was allowed to settle. In each case, some 12 primary fractions collected by repetition of this procedure were refractionated to provide 3 or 4 sharper secondary fractions. These were dissolved in benzene and freeze-dried.

Three polymer preparations, designated 10-71, 9-68, and 8-73 are discussed in the following. They differ in molecular weight, sample 10-71 being the lowest polymër. The fraction designation is added to the polymer code: 10-71; 4B, for example, denoting the second secondary fraction (B) of the fourth primary fraction of the polymer 10-71.

Reagent-grade tetrahydrofuran (THF), containing about 0.025% inhibitor

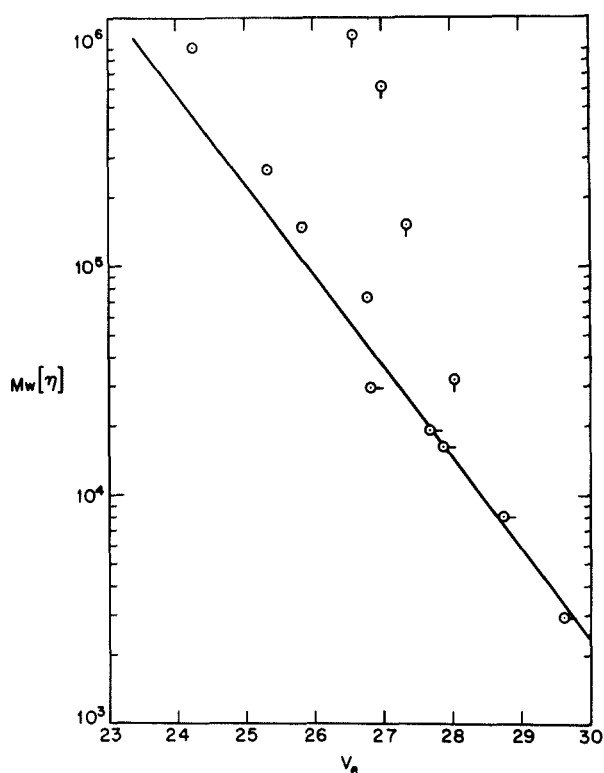


FIG. 1. Dependence of $M_w[\eta]$ on elution volume for fractions from polyphenylene samples 9-68 (\bigcirc), 10-71 (\bigcirc -), and 8-73 (\bigcirc). The solid line is the calibration curve established with narrow distribution polystyrene.

(butylated hydroxytoluene), was used for exclusion chromatography, osmometry, viscometry, and light scattering. Reagent-grade toluene and benzene and redistilled quinoline and cyclohexanone were also used for viscometry. Reagent-grade dimethyl phthalate was the solvent for fluorescence depolarization measurements.

Exclusion chromatography

A Waters Associates analytical gel-permeation chromatograph was used to characterize the fractions. Four Styragel columns with nominal pore-size ratings of 10^3 , 10^4 , 1.5×10^5 , and 3×10^6 were put in series in this order. The elution volume V_e corresponding to the maximum in the refractive index of the effluent was determined from the recorded output of the refractometer incorporated in the instrument. The column set was calibrated by correlating the product of molecular weight M and intrinsic viscosity $[\eta]$ with elution volume using plots of $\log \{M[\eta]\}$ versus V_e for linear narrow-distribution polystyrene [4]. The calibration so obtained [5] is shown in Figure 1.

Elution was carried out with tetrahydrofuran at a flow rate of 1 ml/min. In every run, 0.5 ml of a 4 g/liter solution was injected. Samples were run in duplicate and gave elution volumes reproducible to 0.12 ml or better. A polystyrene sample was injected at intervals to confirm that column characteristics had not changed with time.

Osmometry

Number-average molecular weights M_n were determined from measurements at 25° with a Mechrolab Model 503 osmometer equipped with a Schleicher and Schuell Type 0-7 membrane. Solutions in THF for these and other measurements were made up by weighing. Weight-volume concentrations c were calculated on the assumption of no volume change on mixing. Concentrations were chosen to give osmotic pressures Π no greater than 3 cm of THF. No diffusion of polymer through the membrane was encountered. Data were analyzed graphically by plotting $(\Pi/c)^{1/2}$ versus c [6]. The dependence was found to be linear, and the plots were extrapolated to $c = 0$ to obtain the molecular weight from the limiting relation $(\Pi/c)_{c=0} = RT/M_n$, in which RT has the usual significance.

Light Scattering

The light-scattering photometer has been described elsewhere [7]. In all measurements, vertically polarized 5461-Å incident light was used with a band-pass interference filter placed before the detector photomultiplier to eliminate any fluorescence scattering. There was no measurable depolarization of scattered light and negligible absorption with the solutions used. A thermostat maintained the sample temperature at 25° within $\pm 0.05^\circ$. Solutions were clarified by filtration through a Gelman Polypore membrane with a 0.4-μm pore-size rating.

The weight-average molecular weight M_w and the light-scattering averages of the second virial coefficient A_2^{LS} and the mean-square molecular radius of gyration $\langle s^2 \rangle_{LS}$ were obtained by analysis of data according to the usual relations [6,8,9]:

$$\lim_{\theta \rightarrow 0} \left[\frac{Kc}{R(\theta, c)} \right] \equiv \frac{Kc}{R(0, c)} = \frac{1}{M_w} + 2A_2^{LS}c + \dots \quad (1)$$

$$\lim_{c \rightarrow 0} \left[\frac{Kc}{R(\theta, c)} \right] \equiv \frac{1}{M_w} \left[1 + \frac{1}{3} \left(\frac{4\pi n}{\lambda} \right)^2 \langle s^2 \rangle_{LS} \sin^2 \frac{\theta}{2} + \dots \right] \quad (2)$$

where K is a constant of the system at a given wavelength and $R(\theta, c)$ is the reduced intensity at concentration c and scattering angle θ . Plots of $Kc/R(\theta, c)$ versus $\sin^2 (\theta/2)$ at fixed concentration were extrapolated to $\theta = 0$ to obtain $Kc/R(0, c)$, and these values were plotted against c to obtain M_w and A_2^{LS} from eq. (1). Similarly, plots of $Kc/R(\theta, c)$ versus c at fixed θ were extrapolated to c

= 0, and the intercepts were plotted against $\sin^2 (\theta/2)$ to obtain $\langle s^2 \rangle_{LS}$. Four concentrations were used in each series. The concentrations were checked by evaporation to dryness.

The refractive index increment dn/dc is needed to calculate K . It was determined for 5461-Å light by using a differential refractometer [7,9]. Values of 0.294 and 0.250 ml/g were found for solutions in THF and benzene, respectively, at 25°.

Viscometry

Suspended-level Ubbelohde viscometers (Cannon Instrument Co.) were used for all measurements with the exception noted below. The viscometers were immersed in a 25° constant temperature bath ($\pm 0.02^\circ$). Data on four concentrations of each sample were plotted against c according to the relations [6]

$$\eta_{sp}/c = [\eta] + k'[\eta]^2c + \dots \quad (3)$$

$$(\ln \eta_{rel})/c = [\eta] - \left(\frac{1}{2} - k'\right) [\eta]^2c + \dots \quad (4)$$

to obtain the intrinsic viscosity $[\eta]$ from the intercepts and k' from the slopes. Here, η_{rel} and η_{sp} are, respectively, t/t_0 and $(t - t_0)/t_0$, with t the flow time of solution and t_0 that of solvent. Flow times were corrected for kinetic energy effects, as necessary. Values of the Huggins constant k' were between 0.4 and 0.5.

Measurements on several polymer fractions with a low-shear viscometer [10] revealed no appreciable effect of rate of shear.

Fluorescence

Absorption and fluorescence spectra of THF solutions of the substituted polyphenylene were obtained, respectively, with a Cary Model-14 spectrophotometer and an Aminco-Bowman fluorometer.

Fluorescence depolarization of solutions of the polyphenylene (1.7 g/liter) in dimethylphthalate was determined with the light-scattering photometer, using vertically polarized 4358-Å incident light and a 4358-Å band-reject interference filter before the detector. An analyzer before the photomultiplier permitted measurement of the vertical (I_{\parallel}) and horizontal (I_{+}) fluorescence intensity components excited by the vertically polarized incident light. Since data analysis required only the dimensionless fluorescence emission anisotropy [11]

$$r = (I_{\parallel} - I_{+})/(I_{\parallel} + 2I_{+}) \quad (5)$$

it was not necessary to have absolute intensities. The fluorescence anisotropy was measured over the temperature interval 25°–150°. The temperature dependence of the solvent viscosity, which is required for analysis of the fluorescence data, was measured with an Ubbelohde viscometer.

TABLE I
Dilute Solution Parameters for Phenyl-Substituted Polyphenylene in
Tetrahydrofuran at 25°

Polymer	$10^{-4}M_w$	$10^{-4}M_n$	$10^{12}\langle s^2 \rangle^{LS}$ (cm ²)	$10^4 A_2^{LS}$ (dl/g ²)	$[\eta]$ (dl/g)
10-71; 4A	3.92	2.37	3.52	2.1	0.785
3	2.96	2.19	3.41	5.4	0.665
4B	2.73	2.15	2.63	4.0	0.601
5B	2.00	1.52	3.39	9.9	0.410
7B	1.13	0.96	1.41	11.8	0.266
8B	—	—	—	—	0.215
9B	—	—	—	—	0.170

DISCUSSION

Molecular Weights and Exclusion Chromatography

Dilute solution characterization results for fractions of polymer 10-71 in THF are collected in Table I.

From Figure 1, it can be seen that exclusion chromatography of fractions of this polymer follows the "universal" calibration [4]: the elution peak volumes V_e correlate with the product $M_w[\eta]$ just as they do for polystyrene. However, fractions from polymers 7-68 and 8-73 deviate systematically from that correlation and from each other. Deviations of this sort suggest an association that occurs at concentrations used in the determination of M_w by light scattering but is absent, or decreased, at the much lower concentration at which polymer is eluted from the chromatographic column. Unless association produces aggregates comparatively stable toward dilution, it might be detected in light-scattering experiments by an apparent dependence of chain dimensions on concentration. Such behavior was sometimes discerned with solutions of polymers 9-68 and 8-73. In some instances, the apparent molecular weight depended on the procedure used in making up the solution, a sign that metastable aggregates had formed.

The chromatogram of unfractionated polymer 10-71 was symmetrical; and the ratio M_w/M_n estimated from the dispersion, ignoring axial diffusion, was 3.9. Polymers 9-68 and 8-73 are apparently of higher molecular weight; the chromatogram of 9-68 was skewed toward high molecular weight and that of 8-73 was bimodal. In view of the presumptive association complicating the behavior of these two polymers, we have concentrated on analysis of data from fractions of polymer 10-71, which appears to be free of this complication.

Molecular Dimensions

The mean-square molecular radius of gyration of the polyphenylene necessarily depends on the proportions of meta and para catenation. The light-scattering data in Table I yield an estimate

$$\langle s^2 \rangle_{LS}/N_z a^2 = 8.5 \pm 1.7 \quad (6)$$

for the characteristic ratio of $\langle s^2 \rangle$ to the root-mean-square end-to-end distance of a hypothetical freely jointed chain of N_z links, each of length a . Here, N_z is taken as the z -average number of backbone phenylenes and hence $a = 4.4 \text{ \AA}$ is the length of a phenylene unit along the chain axis. The value of N_z was estimated from M_n and M_w on the assumption that the Schulz-Zimm distribution function [8] applies, i.e., that $N_z = M_z/167 = M_w(h+2)/167(h+1)$, where $h = M_w/M_n$. The ratio $\langle s^2 \rangle_{LS}/N_z$ is sensibly equivalent to $\langle s^2 \rangle/N$ for the homogeneous polymer with $N = N_z$ [9].

Equation (6) is to be compared with what would be expected for all-para catenation (a rigid rod)

$$\langle s^2 \rangle / Na^2 = N/12 \quad (7)$$

and for meta catenation of the two disposable bonds in each repeat unit. In the latter case, the chain is a sequence of links alternating in length, $l = 2a$ and $m = 3a$, joined by a valence angle $\pi - \alpha$ of $2\pi/3$ radians, which gives, for large N [12],

$$\langle s^2 \rangle = \frac{2N}{5} \left(\frac{l^2 + m^2}{12} \right) \left[\frac{1 + \cos \alpha}{1 - \cos \alpha} - \frac{2(l-m)^2}{l^2 + m^2} (\cos \alpha + \cos^3 \alpha) \right] \quad (8)$$

$$\langle s^2 \rangle / Na^2 = 1.258 \quad (9)$$

where N is still the number of phenylene units in the chain. Consequently, we must explain a characteristic size parameter that appears to be independent of chain length, as with the all-meta model, but has a value much larger than the predicted value. Granting free rotation about the axis of the unsubstituted phenylene unit, we approach the problem by assuming that the experimental $\langle s^2 \rangle / Na^2$ results from a random distribution of para and meta linkages occurring with respective probabilities p and $1-p$ at the disposable sites.

Two variants of this kind of model are of interest. First we represent the chain by $n = 5N/2$ equivalent bonds of mean-square length $\langle l^2 \rangle = \frac{1}{2}[(2a)^2 + (3a)^2]$ connected by valence angles $\pi - \alpha$, where α is zero or $\pi/3$ with probabilities p and $1-p$. For large n we then have

$$\langle s^2 \rangle = n \langle l^2 \rangle \left(\frac{1 + \langle \cos \alpha \rangle}{1 - \langle \cos \alpha \rangle} \right) \quad (10)$$

and thus

$$\frac{\langle s^2 \rangle}{Na^2} = \frac{13}{30} \left(\frac{1 + \langle \cos \alpha \rangle}{1 - \langle \cos \alpha \rangle} \right) \quad (11)$$

with

$$\langle \cos \alpha \rangle = (1 + p)/2 \quad (12)$$

For the second, and more realistic, calculation we let bonds of mean-square length $\langle l^2 \rangle$ comprising segments with all-para catenation be connected by a valence angle $\pi - \alpha = 2\pi/3$. Then, the assumption of randomness in the dis-

tribution of meta and para linkages permits calculation of $\langle l^2 \rangle$. For example, the probability that a straight sequence is terminated at length $2a$ or $3a$ is $1 - p$; the probability of termination at $4a$ is zero; the probability of termination at $5a$ is $2p(1 - p)$; etc. In this way the asymptotic relation for large n

$$\begin{aligned} \frac{\langle l^2 \rangle}{a^2} &= \frac{(1-p) [(2^2 + 3^2) + 2(5^2)p + (7^2 + 8^2)p^2 + 2(10^2)p^3 + \dots]}{2(1-p) [1 + p + p^2 + p^3 + \dots]} \\ &= \frac{1}{2} (1-p) \sum_{n=0}^{\infty} [(2+5n)^2 p^{2n} + (3+5n)^2 p^{2n} + 2(5n)^2 p^{2n-1}] \quad (13) \end{aligned}$$

is generated. Completion of the summation then gives

$$k \equiv \frac{\langle l^2 \rangle}{a^2} = \frac{1}{2} (1-p) \left[\frac{13}{(1-p^2)} + \frac{50p^2}{(1-p^2)^2} + \frac{50p(1+p^2)}{(1-p)(1-p^2)^2} \right] \quad (14)$$

To calculate $\langle s^2 \rangle$ from $\langle l^2 \rangle$, we require the number n of effective bonds. We use the Kuhn approximation [6] $Na = n\langle l^2 \rangle^{1/2}$ to obtain n in terms of N , whence with eq. (10) we find

$$\frac{\langle s^2 \rangle}{Na^2} = \frac{\langle l^2 \rangle}{Na^2} \left(\frac{1 + \cos \alpha}{1 - \cos \alpha} \right) = \frac{k^{1/2}}{2} \quad (15)$$

Equations (11) and (15) afford estimates of $\langle s^2 \rangle / Na^2$ that agree within 2% over the range $0.1 \leq p \leq 1$. We note too that eqs. (11) and (15) give $\langle s^2 \rangle / Na^2$ equal to 1.300 and 1.275, respectively, for the all-meta chain, in excellent agreement with the exact result, eq. (9). Figure 2 is a plot of $\langle s^2 \rangle / Na^2$ as a function of the fraction of meta links that serves for either relation. Comparison with the experimental radii of gyration for fractions of polymer 10-71 indicate that 80% ($\pm 5\%$) of the placements are para. At this level $\langle l^2 \rangle^{1/2}$ is $16.8a$, or 75 \AA . It is, of course, this large effective bond length that causes $\langle s^2 \rangle$ to be so large for these relatively low-molecular-weight polymers.

Since these results are unlike model compound data [3] in showing a preference for para catenation, one might question whether $\langle s^2 \rangle / Na^2$ should in fact be given by a relation derived for indefinitely long chains. Some indication of the soundness of this approximation is given by the complete expression [14] for the radius of gyration of a chain with fixed angles $\pi - \alpha$ and links of fixed length l

$$\langle s^2 \rangle = \frac{nl^2}{6} \left(\frac{1+q}{1-q} \right) S(n,q) \quad (16)$$

with $q = \cos \alpha$ and

$$\begin{aligned} S(n,q) = \frac{n+2}{n+1} \left\{ 1 - \frac{6q}{(n+1)(1-q^2)} \left[1 - \frac{2q}{(n+1)(1-q)} \right. \right. \\ \left. \left. + \frac{2q^2(1-q^n)}{n(n+1)(1-q)^2} \right] \right\} \quad (17) \end{aligned}$$

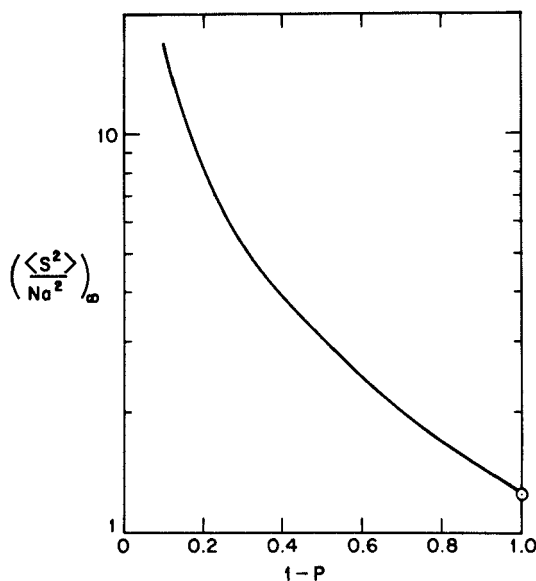


FIG. 2. Characteristic chain dimension for phenyl-substituted polyphenylene calculated from eq. (15) versus the fraction of meta catenation.

It is readily shown [15] that $\langle s^2 \rangle/n$ is within 20% of its limiting value $l^2(1+q)/(1-q)$ if $(1-q)n/q > 10$. For all the polymers discussed here, this parameter, estimated with $n = N/k^{1/2}$, meets the requirement. Hence the experimental result that $\langle s^2 \rangle/Na^2$ is constant is consistent with eq. (17).

Data on fractions of polymers 9-68 and 10-73 have not been included in the analysis above. Values of $\langle s^2 \rangle_{LS}/N_z a^2$, and even $\langle s^2 \rangle_{LS}/N_w a^2$, for these materials are in the range 1.2-4, much smaller than the value 8.5 found for the fractions of 10-71. Together with the chromatographic elution data, we take this to indicate the presence of metastable aggregates of more compact conformation than the unassociated chains, perhaps resembling randomly branched polymer, and not as evidence of greater meta catenation in these polymers.

The model we have used to rationalize the radius-of-gyration data also serves to explain why the polyphenylene exhibits no depolarization of Rayleigh scattering, even though the optical anisotropy δ_0 of the long effective chain links is probably large. Benoit [13] has calculated the anisotropy δ of a chain with free rotation about fixed valence-bond angles:

$$\delta^2 = \frac{\delta_0^2}{n} \left[\frac{1+b}{1-b} - \frac{2b(1-b^n)}{n(1-b)^2} \right] \quad (18)$$

where $b = (3q^2 - 1)/2$. It turns out that for practical purposes δ^2/δ_0^2 can be represented very well as a single-valued function of $n(1-q)/q$. For $n(1-q)/q > 0$, δ^2 is smaller than δ_0^2 by at least a factor of 10; hence, an inconsequential experimental magnitude of δ^2 is reasonable.

Second Virial Coefficient

Values of the second virial coefficient defined by eq. (1) as half the initial slope of $Kc/R(0,c)$ versus c are given in Table I for fractions of polymer 10-71. The magnitudes are of the order expected for ordinary polymers in good solvents. It will also be noted that A_2^{LS} decreases as molecular weight increases. Qualitatively, this is the behavior expected for solutions in a thermodynamically "good" solvent; but the rate of decrease is much greater than is found with typical flexible-chain species: a dependence roughly on $M^{-1.3}$ here as compared with perhaps $M^{-0.3}$ in extreme cases with vinyl polymers [16]. However, since the polyphenylene chains are short in terms of numbers of effective links, this difference need not, of itself, be cause for surprise. For the same reason, theoretical deductions [17a,18] of the asymptotic dependence of A_2 on molecular weight would hardly seem pertinent.

The other information from light scattering listed in Table I can be combined with the second virial coefficient to obtain the quantity

$$\Psi = A_2^{\text{LS}} M_w^{1/2} (\langle s^2 \rangle_{\text{LS}} / M_w)^{-3/2} \quad (19)$$

This falls in the range 0.05×10^{24} – 0.08×10^{24} for the polyphenylene fractions, in marked contrast to the much larger limiting experimental value $\Psi_\infty = 4.0 \times 10^{24}$ attained for monodisperse, linear, flexible-chain polymers in good solvents [17b,19]. To develop a tentative interpretation for this small Ψ , we recall that interaction between a pair of chain segments is characterized by an excluded volume integral [17c] that has a larger positive value, the "better" the solvent for a given polymer. The net repulsion between segments in a good solvent is manifested by an expansion $\alpha^2 \equiv \langle s^2 \rangle_0$ and by a positive second virial coefficient. The well-known perturbation treatment [17a, 17c] of both effects gives α^2 and A_2 as series expansions, for homogeneous polymer,

$$\alpha^2 = 1 + (134/105)z + O(z^2) \quad (20)$$

and

$$A_2 = 4\pi^{3/2} N_A B [1 - 2.865z + O(z^2)] \quad (21)$$

in powers of the variable

$$z = B(\langle s^2 \rangle_0 / M)^{-3/2} M^{1/2} \quad (22)$$

In these equations N_A denotes Avogadro's number and B is proportional to the excluded volume integral. Eliminating z between the two series, Zimm, Stockmayer, and Fixman [20] obtained A_2 as a function of $(\alpha^2 - 1)$, i.e., in linear approximation

$$A_2 M^{1/2} = 4(105/134)\pi^{3/2} N_A [\langle s^2 \rangle_0 / M]^{3/2} (\alpha^2 - 1) \quad (23)$$

Although it is formally limited to $\alpha^2 \approx 1$, eq. (23) correlates typical experimental data surprisingly well over a wide range of α and A_2 . It can be recast in the form

$$\alpha^2 \Psi = 1.05 \times 10^{25} (\alpha^2 - 1) \quad (24)$$

If we accept this relation, ignoring polydispersity as a first approximation, we must conclude that α for the 10-71 fractions is never greater than 1.01. Then the excluded volume parameter z according to eq. (20) is always less than 0.01, and B is simply $A_2/4N_A\pi^{3/2}$. This means that there is virtually no intramolecular excluded volume effect and $\langle s^2 \rangle$ is indistinguishable from the unperturbed dimension, despite a large B , which is expressed in the intermolecular interactions measured by A_2 . In other words, the experimental data on the polyphenylenes are explicable on the basis of an intramolecular excluded volume effect that is small because of a very large unperturbed chain dimension, not because of a small excluded-volume integral. This rationale has also been proposed to account for the similar behavior of cellulose acetate and other cellulose esters in solution [21].

Intrinsic Viscosity

The molecular-weight dependence of the intrinsic viscosity of polyphenylene fractions is shown in Figure 3 (some of the data are included in Table I). It is evident that $[\eta]$ is proportional to M_w determined by light scattering for fractions of polymer 10-71, but the other samples deviate markedly from this correlation. If the chain conformation in these polymers is essentially unperturbed, the proportionality between $[\eta]$ and M_w implies that the hydrodynamic behavior approximates the "free draining" limit. For this case, the bead-and-spring chain model gives [6b, 17d]

$$[\eta] = \pi \langle s^2 \rangle d_s / 200 m_s; \quad d_s = \zeta_0 / 3\pi\eta_0 \quad (25)$$

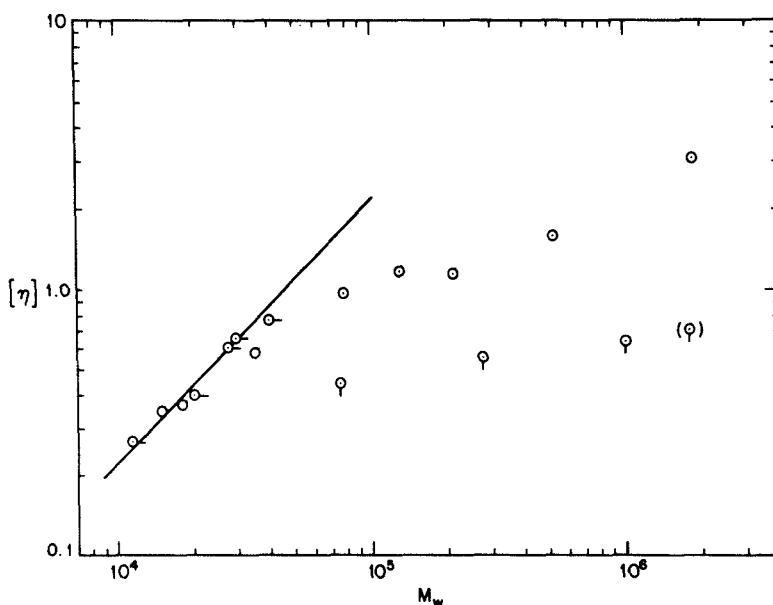


FIG. 3. Intrinsic viscosity versus M_w for polyphenylene fractions. Data points are designated as in Figure 1.

where ζ_0 is the friction factor for an effective hydrodynamic unit of mass m_s and Stokes diameter d_s , and η_0 is the solvent viscosity. In this model the frictional forces arise at beads of diameter d_s separated by a mean-square distance $b^2 = 6\langle s^2 \rangle/n'$, where n' is the number of links in an equivalent freely-jointed chain with $\langle s^2 \rangle$ matching the value for the real chain. For comparison with experiment we use a form of eq. (25) corrected [19], approximately, for polydispersity:

$$\frac{[\eta]}{M_w} = \frac{\pi d_s}{200 m_s} \left(\frac{\langle s^2 \rangle_{LS}}{M_z} \right) \quad (26)$$

With the Kuhn approximation, $n'b = N_z a$, and the experimental $\langle s^2 \rangle_{LS}$, we obtain $b = 224 \text{ \AA}$, or an averaged link length containing 51 backbone phenylene groups. The experimental parameters $[\eta]/M_w = 2.17 \times 10^{-5}$ and $\langle s^2 \rangle_{LS}/M_z = 9.84 \times 10^{-17}$ then give $d_s = 20 \text{ \AA}$.

The artificiality of this model is revealed in the value of d_s , which cannot be associated with a molecular dimension. Similar difficulties have been encountered in studies of cellulose esters [21] and heterocyclic flexible-chain polymers [22]. Consequently, indiscriminate use of eq. (25) to estimate chain dimensions from viscometric data cannot be advised. We observe, however, that if we arbitrarily take m_s as the mass of the 75- \AA effective link for the free rotation model and use the experimental $[\eta]$ and $\langle s^2 \rangle_{LS}$ in eq. (26), we obtain $d_s = 6.8 \text{ \AA}$, a number in plausible correspondence with a chain diameter.

The effects of association, already noted, are evident in the viscosity data on fractions from polymers 9-68 and 8-73. Intrinsic viscosities are much smaller than would be expected by comparison with the "well-behaved" 10-71 series. Moreover, the Mark-Houwink-Sakurada exponent $d \ln [\eta]/d \ln M$ is less than 0.5 for both polymers. These effects are consistent with the presence of aggregates with conformations resembling randomly branched chains [21].

Since exclusion chromatography is carried out at much lower polymer concentration than light scattering and viscometry and any reversible aggregation tends to disappear with decreasing concentration, it is of some interest to obtain a molecular weight M_e from the elution volumes of the 9-68 and 8-73 fractions, assuming that the universal calibration shown in Figure 1 together with the proportionality between $[\eta]$ and M_w shown in Figure 3 holds for these polymers in terms of the molecular weights of species existing in the column. Then, comparing the light scattering M_w with M_e , we could obtain some indication of the minimum degree of association under the conditions of the light-scattering experiments. In this way it is deduced that the aggregates apparently comprise two to five chains, at least, for fractions of polymer 9-68 and from 3 to 36 chains for fractions of 8-73.

Pursuing this line of thought to even more speculative lengths, we can use the M_e calculated as just described and suppose that the aggregates exhibit the viscometric behavior of free-draining branched coils; i.e., the intrinsic viscosity is given by eq. (25) in terms of $\langle s^2 \rangle$ of the aggregate. In this case the degree of association ν can be obtained from

$$[\eta] \approx 2.17 \times 10^{-5} g \nu M_e \quad (27)$$

where g , the ratio of radii of gyration of branched and linear species of the same mass, is a function of branching topology and the frequency of branch nodes. Using values of g for random tetrafunctional branching given by Zimm and Stockmayer [23] with out experimental viscosities, we find the apparent ν to be in the range 0.5–1 for the fractions of polymers 9-68 and 8-73. Since concentrations are higher in viscometry than in light scattering, it is surprising that this result is contrary to the other, more direct, evidences of association. However, it bears emphasis that the argument by which it was reached is tenuous. It ignores possible heterogeneity of aggregates and would be vitiated if their conformation were far from the random coil or if free-draining behavior did not apply, owing to their enhanced segment density.

Fluorescence

The absorption spectrum of a THF solution of the polyphenylene (0.04 g/liter, 10.05-mm path length) shows broad absorption maxima at 305, 285, and 276 nm, and absorption increasing below 230 nm. Irradiation of a solution (6×10^{-4} g/liter) in THF at 305 nm produces intense fluorescence with a maximum at 365 nm. Excitation at 285 or 276 nm produces only weak fluorescence, but this also peaks at 365 nm. The fluorescence is independent of molecular weight.

The fluorescence emission anisotropy r defined by eq. (1) is a measure of the depolarization of the fluorescence. The experiment has the advantage of simplicity, but it is seriously limited with regard to quantitative interpretation for lack of a satisfactory theory relating r to macromolecular properties. For rigid particles with rotatory diffusion constant D_r , the fluorescence anisotropy is given by [11]

$$r = r_0 / (1 + 6D_r\tau) = r_0 / (1 + 3\tau/\rho) \quad (28)$$

where τ is the lifetime of the excited state and $\rho = 1/2D_r$ is the rotatory relaxation time. The intrinsic emission anisotropy r_0 , the limit of r as $D_r\tau$ vanishes, is determined by the angle β between absorption and emission vectors:

$$r_0 = (3 \cos^2 \beta - 1)/5 \quad (29)$$

and thus lies between -0.2 and 0.4 . Using the relation

$$D_r = RT/4M\eta_0[\eta] \quad (30)$$

for a polymer chain rotating as a unit, we can put eq. (28) in the form

$$\frac{1}{r} = \frac{1}{r_0} + \frac{3}{200r_0} \left(\frac{\tau RT}{M\eta_0[\eta]} \right) \quad (31)$$

No adequate theory exists to relate r to the properties of chain molecules with a multiplicity of internal normal modes, but it has been suggested [24] that eq. (28) be modified by putting it in a form that typically appears in the analysis of systems characterized by a distribution of relaxation times:

$$r = r_0 \sum \frac{A_i}{1 + 3\tau/\rho_i} \quad (32)$$

The A_i are a normalized set ($\sum A_i = 1$) of weighting factors for the modes with relaxation times ρ_i . If every term $3\tau/\rho_i$ and the sum $3\tau\sum A_i\rho_i$ are small compared with unity, eq. (32) can be simplified [24]:

$$r \approx r_0 \left[2 + 3\tau \sum_i A_i/\rho_i \right]^{-1} \quad (33)$$

Further if the ρ_i are expressed in terms of dimensionless quantities λ_i

$$\rho_i = 100M\eta_0[\eta]/RT\lambda_i \quad (34)$$

we obtain from eq. (33)

$$\frac{1}{r} = \frac{1}{r_0} + \frac{3\sum A_i\lambda_i}{100r_0} \left(\frac{\tau RT}{M\eta_0[\eta]} \right) \quad (35)$$

where $\sum A_i\lambda_i$ is just a number that correlates r with the experimental variables. Equation (35) is of the same form as eq. (31) for a rigid body. Thus, a plot of r^{-1} versus $\tau RT/M\eta_0[\eta]$ should extrapolate linearly to an intercept r_0^{-1} , and one might hope to learn something about internal molecular dynamics from slope, i.e., from comparison of the apparent value of $\sum A_i\lambda_i$ with values given by possible theoretical models and with the rigid-body relation in eq. (31).

To carry out such an analysis, we need to know the lifetime τ . For the polyphenylene this was determined to be 4.92 nsec by an independent measurement of fluorescence decay. The emission intensity curve $I(t)$ after excitation by a pulse was fitted by an exponential decay function

$$I(t) = I_0 e^{-t/\tau} \quad (36)$$

in time t . Instrumentation and numerical deconvolution techniques used in this method are described elsewhere [25].

A plot of r^{-1} is shown in Figure 4(a) for fractions of polymer 10-71 in dimethyl phthalate over the temperature range 25–150°. The straight line drawn through the data gives $r_0 = 0.314$ and a slope of 0.653, which corresponds to $\sum A_i\lambda_i = 6.85$, according to eq. (35). The slope is much greater than the value 0.047 predicted by eq. (31) with $r_0 = 0.314$. Of course, the failure of the rigid-body model is hardly surprising in view of the flexibility of the polyphenylene chain. Nonetheless, the reasonable correlation of $r^{-1}\tau RT/M_w\eta_0[\eta]$ does suggest that long-range motions of the chain are important, as compared, for example, with side-chain relaxations.

The magnitudes of the experimental fluorescence anisotropy parameters, however, raise further questions about the analysis. The value of r_0 is unexpectedly small. If, as we suppose, the absorption and emission vectors both lie along the axis of the rodlike chain segment, β in eq. (9) is zero, and r_0 should be 0.4. We also note that if $\sum A_i = 6.85$, the condition that $3\tau\sum A_i/\rho_i \ll 1$ fails when $\tau RT/M\eta_0[\eta]$ is greater than about unity. Consequently, most of the experimental data in Figure 3(a) fall outside the range of the independent variable where the linear relation in eq. (35) can be expected to hold, and the extrapolation to $1/r_0$ may be much more hazardous than appears at first sight.

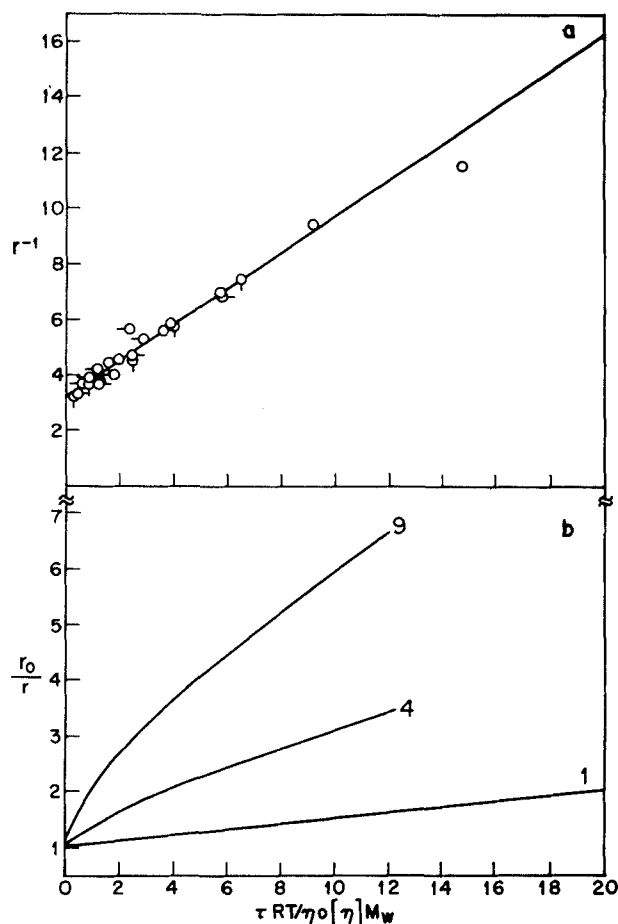


FIG. 4. (a) Reciprocal emission anisotropy r^{-1} for fractions of sample 10-71. (b) r_0/r calculated with eq. (32) as described in the text for $N = 1, 4, 9$.

To assess this extrapolation hazard, it is instructive to consider an illustrative example of the effect of a distribution of relaxation times. For this purpose we suppose there are N equally weighted modes ($A_i = 1/N$) with $\lambda_i = (\pi^2/6)i^2$, ($i = 1, 3, \dots, N$), corresponding to the N longest relaxation times for the Rouse model [17d]. For this case, eq. (35) becomes

$$\frac{1}{r} = \frac{1}{r_0} + \frac{\pi^2(N+1)(2N+1)}{1200r_0} \left(\frac{\tau RT}{M\eta_0[\eta]} \right) \quad (37)$$

which may be compared with r^{-1} calculated directly from eq. (32) with eq. (34). Curves from the latter calculation are shown in Figure 4(b) for N equal to 2, 4, and 9. It is evident that when N is 7 or 9, the limiting linear relation in eq. (37) agrees with the curves only when $\tau RT/M\eta[\eta]$ is too small to be experimentally

accessible. However, the curvature of the plots is so gentle that experimental points might easily be taken to lie on a straight line. Then, a plausible empirical fitting with the form of eq. (35) would give values of $\Sigma A_i \lambda_i / r_0$ and of r_0 that are too small. As an exercise in curve fitting, the experimental data in Figure 7(a) can be accommodated to eq. (33) with the choice of the λ_i and A_i specified above to give $\rho_0 = 0.4$ with $N \approx 5$. The arbitrary character of the calculation makes it impossible to take this result seriously except to indicate the hazard in using eq. (35) to analyze data on flexible chains.

CONCLUSIONS

Our solution measurements are consistent with polyphenylene chains characterized by rodlike segments of average length 70–75 Å joined by 120° valence angles. The large segment length causes the reduced radius of gyration $\langle s^2 \rangle_0 / M$ to be very large. As a consequence, intramolecular volume exclusion effects on chain conformation are negligible, even though interactions evidenced by the positive second virial coefficient do not vanish. Analogous behavior together with a large $\langle s \rangle_0 / M$ is well known for cellulose derivatives.

The large chain dimension of the polyphenylene is also responsible for free-draining hydrodynamic behavior; i.e., the Mark-Houwink-Sakurada exponent is unity, despite the lack of appreciable intramolecular volume exclusion. Again such behavior is characteristic of cellulose derivatives.

Finally, although fluorescence anisotropy data do suggest the importance of dynamic modes involving concerted motions of extensive parts of the polymer chain, the theoretical development is too crude to permit quantitative interpretation.

On the whole, we must regard our conclusions tentative rather than definitive for at least three reasons. (1) The data are limited to a small number of available samples. (2) The statistical theories interrelating conformational, hydrodynamic, and thermodynamic behavior are all for chains comprising large numbers of statistical segments, but the polyphenylene chains are quite short in this sense. (3) Since the problem of intermolecular association frustrated interpretation of data on some polymer preparations, the assumption that aggregates are completely absent in the "well-behaved" samples is obviously problematical.

This study was supported by Grants GP-28538X and DMR74-14953 of the National Science Foundation. J.L.W. acknowledges the support of the Armstrong Cork Company, which made possible his appointment as a Visiting Fellow at Carnegie-Mellon University. Dr. L. K. Patterson obtained the data on fluorescence decay. Assistance on certain phases of the study was rendered by R. W. Nelb and Dr. G. K. Noren, of the University of Iowa, and by S. M. Liwak.

REFERENCES

- [1] G. K. Noren and J. K. Stille, *J. Polym. Sci. Part D*, **5**, 385 (1971).
- [2] *J. Polym. Sci. Part B*, **7**, 525 (1969); J. K. Stille and G. K. Noren, *Macromolecules*, **5**, 49 (1972).
- [3] H. Mukamal, F. W. Harris, and J. K. Stille, *J. Polym. Sci. Part A-1*, **5**, 2721 (1967).

- [4] Z. Grubisic, P. Rempp, and H. Benoit, *J. Polym. Sci. Part B*, **5**, 753 (1967).
- [5] G. C. Berry, *J. Polym. Sci. Part A-2*, **9**, 687 (1971).
- [6] P. J. Flory, "Principles of Polymer Chemistry," Cornell University Press, Ithaca, 1953, (a) Chap. 7; (b) Chap. 14.
- [7] G. C. Berry, *J. Chem. Phys.*, **44**, 4550 (1966).
- [8] B. H. Zimm, *J. Chem. Phys.*, **16**, 1099 (1948).
- [9] E. F. Casassa and G. C. Berry in "Polymer Molecular Weights," P. E. Slade, Jr., Ed., Dekker, New York, 1975, Chap. 5.
- [10] G. C. Berry, *J. Chem. Phys.*, **46**, 1338 (1967).
- [11] D. J. R. Laurence, in "Physical Methods in Macromolecular Chemistry," B. Carroll, Ed., Dekker, New York, 1969, Chap. 5.
- [12] M. V. Volkenstein, "Configurational Statistics of Polymer Chains," Engl. Trans. by S. N. Timasheff and M. J. Timasheff, Wiley-Interscience, New York, 1963, p. 195.
- [13] H. Benoit, C. R. *Acad. Sci.*, **236**, 687 (1953).
- [14] H. Benoit and P. M. Doty, *J. Phys. Chem.*, **57**, 958 (1953); R. A. Sack, *Nature*, **171**, 310 (1953).
- [15] G. C. Berry, *J. Polym. Sci. Polym. Symp.*
- [16] E. F. Casassa, *Polymer*, **3**, 621 (1962).
- [17] H. Yamakawa, "Modern Theory of Polymer Solutions," Harper and Row, New York, 1971, (a) Chap. 4; (b) Chap. 7; (c) Chap. 3; (d) Chap. 6.
- [18] M. Daoud, J. P. Cotton, et al., *Macromolecules*, **8**, 804 (1975).
- [19] G. C. Berry and E. F. Casassa, *J. Polym. Sci. Part D*, **4**, 1 (1970).
- [20] B. H. Zimm, W. H. Stockmayer, and M. Fixman, *J. Chem. Phys.*, **21**, 1716 (1953).
- [21] D. W. Tanner and G. C. Berry, *J. Polym. Sci. Polym. Phys. Ed.*, **12**, 941 (1974).
- [22] G. C. Berry, *Discuss. Faraday Soc.*, **49**, 121 (1970).
- [23] B. H. Zimm and W. H. Stockmayer, *J. Chem. Phys.*, **17**, 1302 (1949).
- [24] M. Frey, P. Wahl, and H. Benoit, *J. Chim. Phys.*, **61**, 1005 (1964).
- [25] L. K. Patterson and E. Vieil, *J. Phys. Chem.*, **77**, 1191 (1973).